

A Theoretic Analysis of a Control System Structure of Towed Underwater Vehicles

Masayoshi Toda

Abstract—In this paper, we present a control system analysis of towed underwater vehicles (TUVs) whose dynamics is extremely complex due to the flexible-cable dynamics and hydrodynamic forces. An explicit state-space representation of the dynamical model is given and, based on it, the fundamental properties such as controllability, observability, and stability are assessed in some details considering a degree of approximation of the cable dynamics, with a numerical and geometric approach. Additionally, we develop some machinery to assess output controllability. The analysis results clarify the significant features of a TUV as a control system and provide useful information for control-system design of TUVs.

I. INTRODUCTION

In this paper, we present an analysis of a control system structure of *towed underwater vehicles* (TUVs), one type of underwater vehicles as shown in Figure 1. TUVs are being applied to exploration and exploitation activities of the underwater environment such as acoustic surveying and mine hunting, and their roles are becoming increasingly important. A TUV has no thruster itself and instead should be driven by a ship through the towline. The TUV considered in this study has maneuverable wings at the middle and rear of the vehicle respectively so as to control its depth and attitude (however, the majority of TUVs practically used have no maneuverable wings).

In these previous years, a lot of papers on control of TUVs have been presented, e.g., [1],[2],[4],[5],[7]–[10], [14],[17]. However, only few papers discussed control problems of TUVs by directly considering their dynamics. One of the most interesting papers is one presented by Campa et al. in 1998 [2] which provided a brief control system analysis and developed a control strategy based on linear H_∞ control powered by some adaptive schemes. However, their emphasis was not on the control system structure, and only preliminary results were then provided on this viewpoint. Therefore, to obtain detailed and better understandings of the fundamental properties of TUVs as a control system, this paper presents a control system analysis of TUVs from some new viewpoints and in some details, using a numerical and geometric approach.

One of the defining features in dealing with control of TUVs is the dynamics of the flexible cable used for towing which leads to an infinite-dimensional problem, while the other feature is highly-nonlinear hydrodynamic forces which every kind of underwater vehicles must be subject to. For over forty years, a lot of research efforts have been devoted to

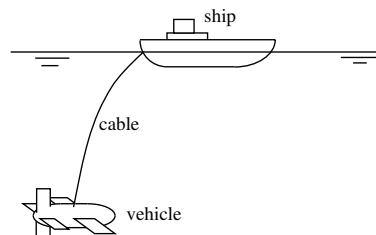


Fig. 1. Schematic diagram of TUV

the dynamics of marine cables, e.g., [15], [6], [3]. Despite the variety of the works, their basic approaches were similarly based on finite-difference methods. In this paper, we take a conventional approach based on finite-dimensional approximation as in those previous papers in both the fields of TUVs and marine cables, and provide an explicit state-space representation of the dynamical model of a TUV. Based on the model, we assess some fundamental properties such as controllability, observability, and stability, and additionally investigate how the number of cable-dimension will affect the control system structure in a numerical manner, which is one feature of our study.

Moreover, we consider not only state controllability but also output controllability which will be shown to be considerably important to the TUV control system. This is the other feature of our study.

Consequently, we shall show that the TUV control system considered in this paper has desirable properties, and clarify its significant features, and provide useful information for control-system design of TUVs.

The remainder of this paper will be organized as follows. In Section II, the problem setting is made and an explicit state-space representation of the dynamical model of the TUV is derived. In Section III, the notion of output controllability is reviewed and some related machinery is developed. In the subsequent section, a control system analysis using this machinery is then presented. In the last section, concluding remarks are given.

II. DYNAMICAL MODEL

A. problem setting

Here, the problem setting and some assumptions for this study are made to make the problem tractable and transparent, and to avoid meaningless complexity. First, we shall restrict ourselves to two-dimensional motions of the TUV as shown in Figure 2, i.e., motions on the vertical plane, throughout this paper, which is the most important problem

M. Toda is with Faculty of Marine Science, Department of Ocean Sciences, Tokyo University of Marine Science and Technology, Konan 4-5-7, Minato-ku, Tokyo, Japan toda@s.kaiyodai.ac.jp

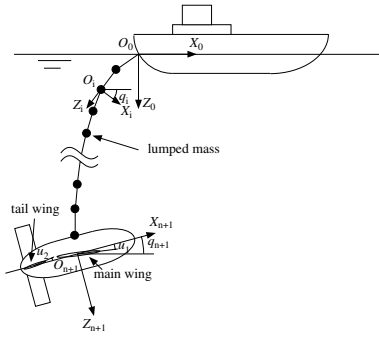


Fig. 2. Configuration of the problem

in a practical use. Further, the following assumptions are made:

- 1) environmental water current such as tide and wave will be ignored,
- 2) the dynamics of the ship towing the vehicle will be ignored and the ship travels only in the horizontal direction,
- 3) the dynamics of the wing actuators will be also ignored,
- 4) the cable (towline) is modeled by a finite number of rigid segments, with their masses lumped on the respective ends, connected by frictionless joints as shown in Figure 2,
- 5) all forces relative to each cable segment are assumed to be applied to its point of mass.

The coordinate systems employed for the problem are shown in Figure 2 where $O_i X_i Z_i$ is for $i = 0$ fixed on the ship with O_0 at its towing point, for $i \in \underline{n}$ on the i th cable segment with O_i at its point of mass, and for $i = n+1$ on the vehicle respectively, where n denotes the number of the cable segments. Each rotation of the coordinate systems is denoted by q_i ($i = 1, \dots, n+1$) defined as in the figure. Further, the maneuverable wings are referred to as the main wing and the tail wing whose angles relative to $O_{n+1} X_{n+1} Z_{n+1}$ are denoted by u_1 and u_2 respectively. Each angle of q_i 's and u_j 's is defined to be positive in the counter-clockwise sense.

B. dynamical model formulation

1) *Lagrange equations of motion*: Based on the above problem setting, a dynamical model formulation is derived. In most of the earlier papers, the dynamical models are represented in the Newton-Euler formulation and the resulting formulae contain the redundant state-variables and the constraint forces explicitly. However, for the purpose of control system analysis and design, the Lagrange approach is more appropriate than the Newton-Euler one. Therefore, we adopt the Lagrange approach so that the resulting formulae contain no redundant state-variable and constraint force.

Note that the system analysis in this paper relies on a numerical method, hence it requires the specific values of the physical parameters. The reference [8] has been so far only one we found where all the values necessary for the

computation of the dynamics are available. Not like other mechanical systems such as a robotic manipulator, it is extremely difficult to suppose some realistic values of the physical parameters for the underwater systems since they involve hydrodynamic parameters. Therefore, we develop the dynamical model so that the resulting dynamics is essentially equivalent to that in the reference [8] and thus we will be able to adopt all the parameters from the reference for our analysis with some minor modification.

First, the inertia matrices are introduced as in the following.

$$M_i = \frac{L(m_c + a_c)}{n} I_2 = m a_c I_2 \quad (1)$$

where M_i for $i \in \underline{n}$ denotes the inertia matrix of the i th cable segment relative to $O_i X_i Z_i$, m_c , a_c , and L denote the mass, the added mass of the cable per unit length, and the total length of the cable respectively. I_k represents the $k \times k$ identity matrix.

M_{n+1} denotes the inertia matrix of the vehicle relative to $O_{n+1} X_{n+1} Z_{n+1}$, each element M_{n+1}^{ij} is as in the following.

$$\begin{aligned} M_{n+1}^{11} &= m_v + a_{v11} \\ M_{n+1}^{12} &= M_{n+1}^{21} = 0 \\ M_{n+1}^{13} &= M_{n+1}^{31} = m_v z_g + a_{v13} \\ M_{n+1}^{22} &= m_v + a_{v22} \\ M_{n+1}^{23} &= M_{n+1}^{32} = -m_v x_g + a_{v23} \\ M_{n+1}^{33} &= J_v + a_{v33} \end{aligned} \quad (2)$$

where m_v , J_v and a_{vij} are the mass, the inertia moment, and the added inertias respectively. (x_g, z_g) represents the coordinates of the center of gravity of the vehicle in $O_{n+1} X_{n+1} Z_{n+1}$.

Let $v_i = (v_{ix}, v_{iz})^T$ (for $i \in \underline{n}$) and $v_{n+1} = (v_{(n+1)x}, v_{(n+1)z}, \dot{q}_{n+1})^T$ denote the velocity vectors corresponding to the respective M_i 's defined in $O_i X_i Z_i$'s. Then, the total kinetic energy K is represented as follows:

$$K = \sum_{i=1}^{n+1} \frac{1}{2} v_i^T M_i v_i. \quad (3)$$

Note that $q = (q_1, \dots, q_{n+1})^T$ can be generalized configuration coordinates for the system and we shall treat the potential forces separately as generalized forces. Thus, the Lagrange equations of motion with (3) yield

$$\frac{d}{dt} \left(\frac{\partial K}{\partial \dot{q}} \right) - \frac{\partial K}{\partial q} = E(q) \ddot{q} + F(q, \dot{q}) = \tau_{bg} + \tau_h \quad (4)$$

where τ_{bg} and τ_h denote the generalized force vectors due to the buoyancy and gravity, and the nonlinear hydrodynamic forces respectively. Each element of positive definite $E(q)$

can be represented as

$$\begin{aligned} E_{ij} &= E_{ji} \\ &= \frac{1}{2} \left(\frac{L}{n} \right)^2 \\ &\quad \cdot \{ (M_{n+1}^{11} + M_{n+1}^{22} + 2k_{ij}ma_c)c(q_i - q_j) \\ &\quad + (a_{v11} - a_{v22})c(q_i + q_j - 2q_{n+1}) \} \\ &\quad \text{(for } i, j \in \underline{n} \text{)} \end{aligned} \quad (5)$$

$$\begin{aligned} E_{i,n+1} &= E_{n+1,i} \\ &= \frac{L}{n} \{ (M_{n+1}^{13} + L_v M_{n+1}^{11})c(q_i - q_{n+1}) \\ &\quad + M_{n+1}^{23}s(q_i - q_{n+1}) \} \\ &\quad \text{(for } i \in \underline{n} \text{)} \end{aligned} \quad (6)$$

$$E_{n+1,n+1} = M_{n+1}^{33} + L_v(2M_{n+1}^{13} + L_v M_{n+1}^{11}) \quad (7)$$

where $c(\cdot)$ and $s(\cdot)$ denote $\cos(\cdot)$ and $\sin(\cdot)$ respectively, $(0, -L_v)$ represents the towing point on the vehicle in $O_{n+1}X_{n+1}Z_{n+1}$ ($L_v > 0$), and k_{ij} denotes the element of the following $n \times n$ matrix:

$$k = \begin{bmatrix} n & n-1 & n-2 & \dots & 1 \\ n-1 & n-1 & n-2 & \dots & 1 \\ n-2 & n-2 & n-2 & \dots & 1 \\ \vdots & \vdots & \vdots & \ddots & 1 \\ 1 & 1 & 1 & \dots & 1 \end{bmatrix}. \quad (8)$$

Next, the Coriolis and centripetal force vector $F(q, \dot{q})$ is represented as in the following.

$$\begin{aligned} F_i &= \sum_{j=1}^n \left[\frac{1}{2} \left(\frac{L}{n} \right)^2 \right. \\ &\quad \cdot \{ (M_{n+1}^{11} + M_{n+1}^{22} + 2k_{ij}ma_c)s(q_i - q_j) \\ &\quad - (a_{v11} - a_{v22})s(q_i + q_j - 2q_{n+1}) \} \dot{q}_j^2 \\ &\quad + \left(\frac{L}{n} \right)^2 (a_{v11} - a_{v22}) \\ &\quad \cdot s(q_i + q_j - 2q_{n+1}) \dot{q}_j \dot{q}_{n+1}] \\ &\quad + \frac{L}{n} \{ M_{n+1}^{23}c(q_i - q_{n+1}) \\ &\quad + (M_{n+1}^{13} + L_v M_{n+1}^{11})s(q_i - q_{n+1}) \} \dot{q}_{n+1}^2 \\ &\quad + \frac{L}{n} (a_{v11} - a_{v22})s(q_i - 2q_{n+1})v_0 \dot{q}_{n+1} \\ &\quad + \frac{1}{2} \left(\frac{L}{n} \right)^2 \{ (a_{v11} - a_{v22})c(q_i - 2q_{n+1}) \\ &\quad + (M_{n+1}^{11} + M_{n+1}^{22} + 2Lk_{1i}ma_c)c(q_i) \} v_0 \\ &\quad \text{(for } i \in \underline{n} \text{)} \end{aligned} \quad (9)$$

$$\begin{aligned} F_{n+1} &= \sum_{i=1}^n \left[\sum_{j=1}^n \left\{ -\frac{1}{2} \left(\frac{L}{n} \right)^2 \right. \right. \\ &\quad \cdot (a_{v11} - a_{v22})s(q_i + q_j - 2q_{n+1}) \dot{q}_i \dot{q}_j \} \\ &\quad - \frac{L}{n} \{ M_{n+1}^{23}c(q_i - q_{n+1}) \\ &\quad + (M_{n+1}^{13} + L_v M_{n+1}^{11})s(q_i - q_{n+1}) \} \dot{q}_i^2 \\ &\quad \left. \left. - \frac{L}{n} (a_{v11} - a_{v22})s(q_i - 2q_{n+1})v_0 \dot{q}_i \right] \end{aligned}$$

$$\begin{aligned} &+ \frac{1}{2} (a_{v11} - a_{v22})s(2q_{n+1})v_0^2 \\ &+ \{ (M_{n+1}^{13} + L_v M_{n+1}^{11})c(q_{n+1}) \\ &+ M_{n+1}^{23}s(q_{n+1}) \} v_0 \end{aligned} \quad (10)$$

where v_0 denotes the velocity of the towing point on the ship in the horizontal direction (recall assumption 2)).

2) *generalized forces*: First, consider τ_{bg} associated with buoyancy and gravity. Let B_c and B_v denote the buoyancy of the cable per unit length and of the vehicle respectively and g be the gravitational acceleration. Then, using the principle of virtual work, τ_{bg} can be obtained as,

$$\tau_{bgi} = \frac{L}{n} \left\{ \frac{Lk_{1i}}{n} (B_c - m_c g) + B_v - m_v g \right\} s(q_i) \quad \text{(for } i \in \underline{n} \text{)} \quad (11)$$

$$\begin{aligned} \tau_{bg n+1} &= (B_v x_b - m_v g x_g)c(q_{n+1}) \\ &\quad + \{ B_v L_v - m_v g(L_v + z_g) \} s(q_{n+1}) \end{aligned} \quad (12)$$

where $(x_b, 0)$ represents the center of buoyancy of the vehicle in $O_{n+1}X_{n+1}Z_{n+1}$.

Next, consider the hydrodynamic force vector τ_h . Let the centers of hydrodynamic force on the main and tail wings be $(0, 0)$ and $(-L_t, 0)$ in $O_{n+1}X_{n+1}Z_{n+1}$ respectively ($L_t > 0$), and let h_{ci} be the drag on the i th cable segment, h_{mD} and h_{mL} be the drag and lift [12] on the main wing. Similarly, the suffix t is for the tail wing, the suffix v for the body of the vehicle, the suffix D for drag and L for lift respectively. Then, we can obtain τ_h in the following form.

$$\begin{aligned} \tau_{hi} &= - \sum_{j=i}^n \frac{L}{n} h_{cj} c(\alpha_i) \\ &\quad + \frac{L}{n} \{ h_{mD} c(\alpha_{n+1} - q_{n+1} + q_i) \\ &\quad + h_{tD} c(\alpha_t - q_{n+1} + q_i) \\ &\quad + (h_{vL} + h_{mL})s(\alpha_{n+1} - q_{n+1} + q_i) \\ &\quad + h_{tL}s(\alpha_t - q_{n+1} + q_i) \} \text{ (for } i \in \underline{n} \text{)} \end{aligned} \quad (13)$$

$$\begin{aligned} \tau_{h n+1} &= h_{mD} L_v c(\alpha_{n+1}) + h_{mL} L_v s(\alpha_{n+1}) \\ &\quad - (h_{tD} L_v + h_{tL} L_t) c(\alpha_t) \\ &\quad + (-h_{tD} L_t + h_{tL} L_v) s(\alpha_t) \\ &\quad + h_{vL} (L_v \sin \alpha_{n+1} + CM) \end{aligned} \quad (14)$$

where CM is a constant parameter associated with hydrodynamic moment and α_i for $i \in \underline{n+1}$ is the angle of attack [12] defined as (recall Equation (3)),

$$\alpha_i = \tan^{-1} \left(\frac{v_{iz}}{v_{ix}} \right) \quad (v_{ix} \neq 0). \quad (15)$$

The angle of attack α_t is similarly defined for the tail wing with the velocity vector denoted by v_t in $O_{n+1}X_{n+1}Z_{n+1}$.

Each of the hydrodynamic forces is a polynomial of each angle of attack, control angle of wing u_i , and velocity

represented as in the following.

$$h_{ci} = \frac{L}{n}(CD_{c1}\alpha_i^2 + CD_{c2})\|v_i\|^2 \quad (16)$$

$$h_{mL} = CL_{m1}(\alpha_{n+1} + u_1 + CL_{m2})\|v_{n+1}\|^2 \quad (17)$$

$$h_{mD} = \{CD_{m1}(\alpha_{n+1} + u_1 + CL_{m2})^2 + CD_{m2}\}\|v_{n+1}\|^2 \quad (18)$$

$$h_{tL} = CL_{t1}(\alpha_t + u_2)\|v_t\|^2 \quad (19)$$

$$h_{tD} = \{CD_{t1}(\alpha_t + u_2)^2 + CD_{t2}\}\|v_t\|^2 \quad (20)$$

$$h_{vL} = CL_{v1}\alpha_{n+1}\|v_{n+1}\|^2 \quad (21)$$

where CD_x and CL_x are constant drag and lift coefficients and $\|\cdot\|$ denotes the Euclidean norm.

3) *control system formulation*: Additionally, we assume that the ship velocity v_0 to be positive constant and choose outputs of the system to be the depth and attitude of the vehicle. Then by some algebraic manipulation to Eq. (4), the above dynamical system can be transformed into the following familiar control-system form,

$$\begin{aligned} \dot{x} &= f(x, u) \\ y &= g(x) \end{aligned} \quad (22)$$

where the input vector $u = (u_1, u_2)^T \in \mathbf{R}^2$, the state vector $x = (x_1^T, x_2^T)^T = (q^T, \dot{q}^T)^T \in$ the state-space manifold $\mathcal{X} \subset \mathbf{R}^{2n+2}$, the output vector $y = (y_1, y_2)^T \in$ the output-space manifold $\mathcal{Y} \subset \mathbf{R}^2$ and the mappings f and g are,

$$f(x, u) = \begin{bmatrix} x_2 \\ E(x_1)^{-1}\{-F(x) + \tau_{bg}(x_1) + \tau_h(x, u)\} \end{bmatrix} \quad (23)$$

$$g(x) = \begin{bmatrix} \frac{L}{n} \sum_{i=1}^n \cos q_i + L_v \cos q_{n+1} \\ q_{n+1} \end{bmatrix}. \quad (24)$$

III. OUTPUT CONTROLLABILITY

In this section, we review output controllability. In practical control problems, we are often interested in only the output rather than the state as long as the whole system can be stabilized. The control of TUVs is exactly the case, which has motivated the present framework.

First, we present the definition of output controllability and then develop some machinery to be exploited to analyze control systems in this framework. The essence of this concept is an issue of how the associated tangent mapping $g_* : T\mathcal{X} \rightarrow T\mathcal{Y}$ of $g : \mathcal{X} \rightarrow \mathcal{Y}$ will map the distribution generated by the inputs on the state-space manifold \mathcal{X} onto the distribution on the output-space manifold \mathcal{Y} .

Definition 1: Consider the system modeled as in the form of Eq. (22) where $u \in \mathcal{U} \subset \mathbf{R}^k$, the admissible control set, $x \in \mathcal{X}$, the state-space C^∞ connected manifold of dimension l , $y \in \mathcal{Y}$, the output-space C^∞ connected manifold of dimension m , and f and g are C^∞ mappings. Suppose $x(0) = x_0$ and $y(0) = y_0 = g(x_0)$ and if the set of points on the output space which can be reached from y_0 by using an input function $u(\cdot) : [0, t] \rightarrow \mathcal{U}$ in a finite time contains a neighborhood of y_0 , then we say the system is output controllable at x_0 . Moreover, if x_0 is an equilibrium with an

input $u_0 \in \mathcal{U}$, i.e., $f(x_0, u_0) = 0$ then we call $y_0 = g(x_0)$ an *output-controllable equilibrium*.

Then, we introduce a sufficient condition for an output-controllable equilibrium of the nonlinear system represented by (22) by using a linearization approach, which is exactly the modification of state-space controllability version in the reference [13]. See the appendix A for the proof.

Proposition 1: Consider the nonlinear system of the form (22) let $x(0) = x_0 \in \mathcal{X}$ and $u(0) = u_0 \in \mathcal{U}$ satisfying $f(x_0, u_0) = 0$. We obtain the linearization of the system at $x = x_0$ and $u = u_0$ as,

$$\begin{aligned} \dot{z} &= \frac{\partial f}{\partial x}(x_0, u_0)z + \frac{\partial f}{\partial u}(x_0, u_0)v \\ p &= \frac{\partial g}{\partial x}(x_0)z \end{aligned} \quad (25)$$

where $v \in \mathbf{R}^k$, $z \in \mathbf{R}^l$ and $p \in \mathbf{R}^m$. Suppose that this linear system is output controllable at $z = 0$, then the original nonlinear system is also output controllable at x_0 , and hence $y_0 = g(x_0)$ is an output-controllable equilibrium.

Finally, we discuss the open property of output-controllable equilibria on the output-space manifold, that is, not being an isolated point. See the appendix B for the proof.

Proposition 2: Consider the nonlinear system (22) again and make the same assumption as in Proposition 1. Additionally, if $\frac{\partial f}{\partial x}(x_0, u_0)$ is non-singular then there exists a neighborhood of $y_0 = g(x_0)$ where every point y is also an output-controllable equilibrium.

Remark: As stated in the reference [13], the above discussions also hold for the time-reversed system, which implies that for any y_1 and $y_2 \in \mathcal{Y}$ there exist admissible control functions such that one can steer from y_1 to y_2 in a finite time and *vice versa*.

IV. ANALYSIS OF CONTROL SYSTEM STRUCTURE

In this section, we present a control system analysis of the dynamical model derived in Section II in a numerical manner. Specifically, we shall investigate the controllability, observability and stability at equilibria of the system, and furthermore discuss the output controllability. Throughout this section, we shall emphasize a point of view how these characteristics of the system will be affected by the number of cable segments, i.e., the order of approximation of the system, to explore the property of the infinite dimensional system. All the parameters and their values used for the analysis are shown on Table 1, most of which are adopted from the reference [8].

A. controllability, observability, and stability

Let us consider the system (22) and its equilibrium with the main wing input $u_1 = 0$ (deg) and the tail wing input $u_2 = -1.568$ (deg) which chosen so that the attitude of the vehicle $q_{n+1} = 0$. For these inputs and several numbers of the cable segments $n = 2, 5, 10, 20$, we obtain the respective equilibria corresponding to n 's and each configuration of them is depicted in Fig. 3.

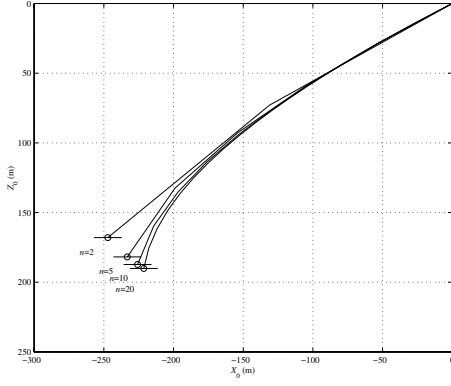


Fig. 3. Equilibriums of TUV system

Then, at each equilibrium, we obtain the linearization represented in the form of (25) with the symbols in (40). To assess the Kalman rank conditions, we construct the following matrices,

$$W_c = [B, AB, \dots, A^{n-1}B] \Lambda_c \quad (26)$$

and

$$W_o = [C^T, A^T C^T, \dots, A^{n-1T} C^T] \Lambda_o \quad (27)$$

where Λ_c and Λ_o are the $2l \times 2l$ non-singular diagonal-scaling matrices so that each non-zero component column vector of W_c and W_o has the magnitude of 1. So, we call W_c the normalized controllability matrix and W_o the normalized observability matrix, and check them by using singular value decomposition as,

$$W_c = U_c \Sigma_c V_c^T \quad (28)$$

$$W_o = U_o \Sigma_o V_o^T, \quad (29)$$

where U_c and U_o are the $l \times l$ orthogonal matrices, Σ_c and Σ_o are the $l \times l$ diagonal matrices with elements of the decreasingly ordered singular values, and V_c and V_o are the $2l \times l$ matrices. By the geometric control theory [16], it is known that the controllable subspace and observable subspace coincide with $Im(W_c)$ and $Im(W_o)$ when Λ_c and Λ_o are identity matrices respectively. Furthermore, it is straightforward to verify that those subspaces are invariant for such scalings.

It is important to note here that the scaling matrices Λ_c and Λ_o will play an important role in our own approach for analyzing the system. The purpose of the application of those matrices is to focus on the geometric structure of the tangent and cotangent vectors in the first term of W_c and W_o , and to ignore the unbalance of their magnitudes. This approach is particularly powerful for high-order systems, which will be discussed later.

First, we take, as an illustrative example, the results of the

case where $n = 2$ (the order of the system $l = 6$),

$$\Sigma_c = \text{diag}[3.416, 0.5752, 5.459 \times 10^{-3}, 4.137 \times 10^{-3}, 7.034 \times 10^{-4}, 1.738 \times 10^{-5}] \quad (30)$$

$$\Sigma_o = \text{diag}[2.992, 1.000, 1.000, 1.000, 0.2131, 2.231 \times 10^{-3}]. \quad (31)$$

As seen from the above, both the matrices are of full rank and hence the system is controllable and observable mathematically. However, we notice that there exists some unbalance among the state subspaces, and therefore expect there exist *hardly controllable* and *hardly observable* subspaces in some sense (Campa et al. also stated this point briefly in [2]). Since in a practical control problem we generally have to limit the control input magnitude and the accuracy of measurements, this point of view will then become important. Note that the similar notion concerning such unbalance of the state space can be found in [11] where their purposes are to develop *balanced realization* and model reduction based on it.

Table 1: Parameters for computation

Symbol	Value	Unit
m_c	0.95	kg/m
a_c	$1.76715\rho \times 10^{-4}$	kg/m
B_c	0.69g	N/m
m_v	182.687	kg
a_{v11}	0.010ρ	kg
a_{v13}	0	kgm
a_{v22}	0.539ρ	kg
a_{v23}	0.032ρ	kgm
a_{v33}	0.039ρ	kgm ²
I_v	26.078	kgm ²
x_g	0.017	m
z_g	0.02	m
x_b	0.017	m
L	300	m
L_v	0.205	m
L_t	0.7	m
CD_{c1}	$-1.23075\rho \times 10^{-3}$	Ns ² /m ³
CD_{c2}	$3.975\rho \times 10^{-3}$	Ns ² /m ³
CL_{m1}	1.72595ρ	Ns ² /m ²
CL_{m2}	-0.141372	rad
CD_{m1}	0.60835ρ	Ns ² /m ²
CD_{m2}	0.0274506ρ	Ns ² /m ²
CL_{t1}	0.09978ρ	Ns ² /m ²
CD_{t1}	$8.11639\rho \times 10^{-3}$	Ns ² /m ²
CD_{t2}	$7.22347\rho \times 10^{-4}$	Ns ² /m ²
CL_{v1}	0.0766708ρ	Ns ² /m ²
CM	1.17268	m
g	9.8	m/s ²
ρ	1025	kg/m ³

Let us focus on the minimum singular value of W_c for example and the associated column vector u_{c6} in U_c which represents the subspace which might be hardly controllable. By computation, we obtain

$$u_{c6} = [0.8334, -0.5371, -0.0002, 0.1077, -0.0733, -0.0001]^T \quad (32)$$

and give some interpretation to this subspace as depicted in Fig. 4 (a). As shown in the figure, this subspace represents

$$\begin{aligned}
\bar{A} &= U_c^T A U_c \\
&= \left[\begin{array}{c|c} \bar{A}_{11} & \bar{A}_{12} \\ \hline \bar{A}_{21} & \bar{A}_{22} \end{array} \right] \\
&= \left[\begin{array}{cccccc|c} -7.854 & 4.894 \times 10^{-1} & 9.991 \times 10 & 3.509 \times 10^3 & -1.257 \times 10^2 & & 8.429 \times 10 \\ 1.548 \times 10^{-1} & 7.489 \times 10^{-2} & -1.469 \times 10 & -4.498 \times 10^2 & 1.848 \times 10 & & -1.239 \times 10 \\ -2.484 \times 10^{-3} & -1.731 \times 10^{-2} & -7.616 & -5.310 & 1.599 \times 10^{-1} & & -1.413 \\ -5.086 \times 10^{-4} & -1.605 \times 10^{-2} & 8.074 \times 10^{-2} & -5.815 \times 10^{-1} & 3.849 \times 10^{-2} & & 8.668 \times 10^{-3} \\ 5.611 \times 10^{-4} & -9.160 \times 10^{-3} & 1.672 \times 10^{-1} & -7.563 \times 10^{-1} & 3.085 \times 10^{-2} & & 3.555 \times 10^{-5} \\ -1.715 \times 10^{-5} & -1.381 \times 10^{-5} & 1.209 \times 10^{-2} & 1.860 \times 10^{-2} & -1.317 \times 10^{-3} & & -3.682 \times 10^{-2} \end{array} \right] \\
\bar{B} &= U_c^T B \\
&= \left[\begin{array}{c} \bar{B}_1 \\ \hline \bar{B}_2 \end{array} \right] \\
&= \left[\begin{array}{cc|c} 6.825 & -7.379 & \\ -1.004 & 1.085 & \\ -4.704 \times 10^{-3} & 1.324 \times 10^{-2} & \\ -2.264 \times 10^{-2} & -1.628 \times 10^{-2} & \\ 1.402 \times 10^{-3} & 1.851 \times 10^{-4} & \\ -4.213 \times 10^{-5} & 8.855 \times 10^{-5} & \end{array} \right] \tag{33}
\end{aligned}$$

$$\begin{aligned}
\bar{C} &= C U_c \\
&= \left[\bar{C}_1 \mid \bar{C}_2 \right] \\
&= \left[\begin{array}{cccc|c} -2.714 \times 10^{-3} & -5.284 \times 10^{-2} & -4.937 & -7.968 & -1.684 \times 10^2 & 4.689 \times 10 \\ -1.455 \times 10^{-1} & -9.893 \times 10^{-1} & 6.884 \times 10^{-4} & 9.823 \times 10^{-3} & -2.298 \times 10^{-4} & -2.070 \times 10^{-4} \end{array} \right] \tag{34}
\end{aligned}$$

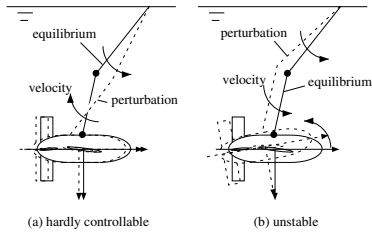


Fig. 4. Particular subsystems of TUV

that q_1 increases, however q_2 decreases, while q_3 stays relatively to the equilibrium, and intuitively we can understand it might be difficult to control such a mode.

Next, we make a coordinate transformation for the linear system by using the orthogonal matrix U_c and the result is as in (33). Note that if the minimum singular value of W_c were really zero then $\bar{A}_{21} = 0$ and $\bar{B}_2 = 0$. Thus, from the above numerical results, we expect the system is close to the uncontrollable system, and hence which also justifies the significance of such a concept.

Let us consider the stability of the equilibrium by checking the eigenvalues of A , $\lambda = \{-7.674 + 0.4249i, -7.674 - 0.4249i, -2.801, 2.214, -0.03969, -0.009737\}$. We notice that λ_4 is a non-oscillatory unstable mode while the others are all stable modes. The associated eigenvector with λ_4 is $[0.2885, 0.7481, -2.547, -106.294, -101.9, -0.4182]^T$

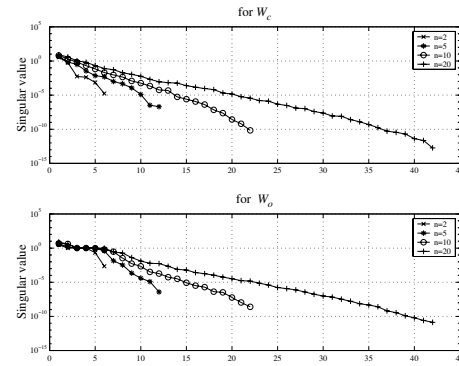


Fig. 5. Singular values of W_c and W_o

whose interpretation can be depicted as in Fig. 4 (b). We can associate this mode with a kite losing its balance.

Here one question arises, whether this unstable mode is contained in the hardly controllable subspace or not? To answer this question, we investigate the respective eigenvalues λ^1 and λ^2 of \bar{A}_{11} and \bar{A}_{22} . Then we obtain $\lambda^1 = \{-7.675 + 0.4251i, -7.675 - 0.4251i, -2.801, 2.214, -0.01012\}$ and $\lambda^2 = -0.03682$ which therefore implies that the unstable mode is not contained in the hardly controllable subspace.

Furthermore, we discuss how all those properties discussed above for $n = 2$ are for a larger number of the cable segments. Figure 5 shows the singular values of W_c and W_o

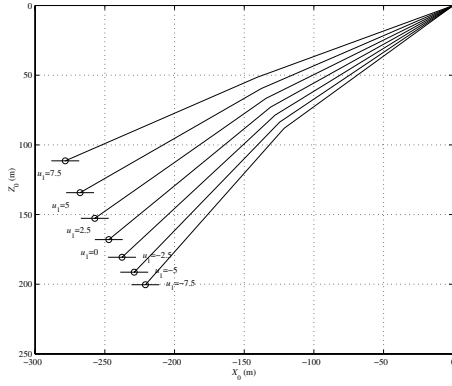


Fig. 6. Equilibria of TUV system

for each n . As seen from the figure, the minimum singular value becomes the smaller with the larger n for both W_c and W_o . In addition, we introduce the fact that the characteristics of hardly controllable and hardly unobservable subspaces and the decomposition based on them become the more prominent for the higher order system. Therefore, we can expect that there exist a hardly controllable and a hardly observable subspaces for the infinite dimensional system in some sense, although it might be difficult to define the term “hardly” uniformly because it will depend on applications.

On the other hand, with respect to the stability, regardless of n , there always exists only one non-oscillatory unstable eigenvalue of near 2 for $n = 2, 5, 10, 20$ and the associated eigenvector v always has the property that v_1, \dots, v_n are positive while $v_{n+1}, \dots, v_{2(n+1)}$ are negative the same as shown for $n = 2$. Furthermore, loosely speaking, this mode is not contained in a hardly controllable subspace nor in a hardly observable subspace. We expect also this fact holds for the infinite dimensional system.

It is important to note again the role of the scaling matrices Λ_c and Λ_o . Without those scalings, the features discussed above will not be prominent for higher order systems such as $n = 20$ in the sense of geometric structure, which is mainly due to the large magnitude of higher order. That’s exactly the reason why we employed this approach. In this paper, we discuss the controllable subspaces from a geometric viewpoint. However, we note that consideration of them with time order together is also important.

B. output controllability

The above discussion on hardly controllability has motivated the notion of output controllability. That is, we are here interested in a question “even if the hardly controllable subspaces are really uncontrollable then is the system still output controllable?” We present an analysis of the TUV system from this point of view by using the machinery developed in Section III.

Again, consider the case $n = 2$ and recall the transformed linearization (33). Similarly in (33) applying U_c to C yields \bar{C} in (34) and thus $\text{rank}(\bar{C}_1) = 2$. Then, the linearization is output controllable at its origin, and therefore from

Proposition 1 we conclude that the TUV system is output controllable in the equilibrium and say that this equilibrium is an output-controllable equilibrium, even if the hardly controllable subspace is really uncontrollable.

Next, by applying Proposition 2 to this output-controllable equilibrium, we discuss its open property. In fact, by computation we can verify that $\frac{\partial f}{\partial x}(x_0, u_0)$ is non-singular. Since we have already shown the system is output-controllable in this equilibrium, then it follows from Proposition 2 that there exists a neighborhood of $y_0 = g(x_0)$ where every point y is also an output-controllable equilibrium.

C. for other equilibria

At the last of this section, we present the results for the other equilibria as depicted in Fig. 6. At each equilibrium the vehicle attitude is 0 (deg), and the respective main wing inputs are -7.5, -5.0, -2.5, 0, 2.5, 5.0, and 7.5 (deg). Consequently, all those properties discussed above for the one equilibrium, i.e., hardly controllable, hardly observable, unstable modes, an output-controllability equilibrium and its open property are invariant for the other equilibria, and moreover, for the system dimensions within our consideration. Therefore, those significant features of this type of TUV control system are expected to be essentially generic ones.

V. CONCLUSION

We have discussed the fundamental control system structure of the TUV system. All those discussions have shown that the TUV has a desirable structure as a control system with respect to (output) controllability, observability and stability. Further, it has been verified that these fundamental properties are invariant for dimensions of approximation for the TUV system and also for equilibria within our consideration. The analysis presented relies on the numerical method and hence the results are dependent on the given specific parameters. However, the TUV considered in this paper is a general type of TUVs and the results are therefore expected to be essentially generic ones, and provide useful information for control-system design of TUVs.

APPENDIX

A. Proof of Proposition 1

Since the linearization Eq. (25) is output controllable at $z = 0$ then for a given time $T > 0$ there exist input functions $v^1(\cdot), \dots, v^m(\cdot)$ such that the corresponding outputs $p^1(T), \dots, p^m(T)$ are independent.

Next, using these inputs $v^i(\cdot)$ ’s for the linear system we construct the inputs for the nonlinear system in the following way,

$$u(t, \xi_1, \dots, \xi_m) := u_0 + \xi_1 v^1(t) + \dots + \xi_m v^m(t), \quad (35)$$

which technique plays a key role in this proof. Briefly, we shall prove that (ξ_1, \dots, ξ_m) can be a coordinate chart of the output-space manifold \mathcal{Y} .

By taking $|\xi_i|$ small enough in $u(\cdot, \xi)$, there will exist the corresponding solutions of the system (22) for all $0 \leq t \leq T$

denoted by $x(t, \xi)$ and $y(t, \xi)$ initiating $x(0, \xi) = x_0$ and $y(0, \xi) = y_0$. Consider now the following mappings,

$$\phi : \xi \mapsto x(t, \xi) \quad \xi \text{ near } 0 \quad (36)$$

$$\psi : \xi \mapsto y(t, \xi) \quad \xi \text{ near } 0, \quad (37)$$

and further the associated tangent mappings ϕ_* and ψ_* in the Jacobian-matrix forms at $\xi = 0$,

$$Z(t) = \left. \frac{\partial x(t, \xi)}{\partial \xi} \right|_{\xi=0} = \frac{\partial x}{\partial \xi}(t, 0) \quad (38)$$

$$\begin{aligned} Y(t) &= \left. \frac{\partial y(t, \xi)}{\partial \xi} \right|_{\xi=0} = \left. \frac{\partial g(x(t, \xi))}{\partial \xi} \right|_{\xi=0} \\ &= \frac{\partial g}{\partial x}(x_0)Z(t). \end{aligned} \quad (39)$$

By substituting $x(t)$ and $u(t)$ by $x(t, \xi)$ and $u(t, \xi)$ in (22) respectively and differentiating (22) with respect to ξ at $\xi = 0$, we obtain

$$\begin{aligned} \dot{Z}(t) &= AZ(t) + B[v^1(t), \dots, v^m(t)] \\ Y(t) &= CZ(t) \end{aligned} \quad (40)$$

where $A = \frac{\partial f}{\partial x}(x_0, u_0)$, $B = \frac{\partial f}{\partial u}(x_0, u_0)$ and $C = \frac{\partial g}{\partial x}(x_0)$. By definition of $v^i(\cdot)$'s, the column vectors of $Y(T) = [p^1(T), \dots, p^m(T)]$ are independent and therefore it follows from the Inverse Function Theorem that (ξ_1, \dots, ξ_m) can be a coordinate chart around y_0 . Hence, the proof is completed.

B. Proof of Proposition 2

Since $\frac{\partial f}{\partial x}(x_0, u_0)$ is non-singular, then it follows from the Implicit Function Theorem that there exist a neighborhood W of (x_0, u_0) , a neighborhood V of u_0 , and a C^∞ mapping $h : V \rightarrow \mathcal{X}$ such that $h(u_0) = x_0$ and

$$\{(x, u) \in W \mid f(x, u) = f(h(u), u) = 0, u \in V\}. \quad (41)$$

Now, let (x, u) be restricted to W and rewrite the equation (39) in the proof of Proposition 1 as in the following.

$$\begin{aligned} Y(t) &= \frac{\partial g}{\partial x}(x_0) \left. \frac{\partial x(t, u(t, \xi))}{\partial u} \right|_{\xi=0} \left. \frac{\partial u(t, \xi)}{\partial \xi} \right|_{\xi=0} \\ &= \frac{\partial g}{\partial x}(x_0) \frac{\partial h}{\partial u}(u_0) \frac{\partial u}{\partial \xi}(t, 0) \end{aligned} \quad (42)$$

where the fact that $x = h(u)$ in W is used, furthermore which implies that the rank of

$$\frac{\partial y}{\partial u}(u_0) = \frac{\partial g}{\partial x}(x_0) \frac{\partial h}{\partial u}(u_0) \quad (43)$$

is m since the rank of $Y(T)$ is m as in the proof of Proposition 1. Hence, there exists a neighborhood U_1 of y_0 such that

$$\{y \in U_1 \mid y = g(h(u)), f(h(u), u) = 0, u \in V\}. \quad (44)$$

On the other hand, recall the matrices $A = \frac{\partial f}{\partial x}(h(u_0), u_0)$, $B = \frac{\partial f}{\partial u}(h(u_0), u_0)$ and $C = \frac{\partial g}{\partial x}(h(u_0))$ of the linearization. By continuity of $h(\cdot)$ and these matrices, it follows that there exists a neighborhood $U_2 \subset U_1$ of y_0 such that every $y \in U_2$ is an output-controllable equilibrium. Hence, U_2 is the desired neighborhood.

REFERENCES

- [1] B. Buckham, M. Nahon, M. Seto, X. Zhao, and C. Lambert, "Dynamics and control of a towed underwater vehicle system, part I: model development," *Ocean Engineering*, 30, pp. 453-470, 2003.
- [2] G. Campa, J. Wilkie and M. Innocenti, "Robust control and analysis of a towed underwater vehicle," *Int. J. Adapt. Control Signal Process.*, 12, pp. 689-716, 1998.
- [3] Z. Feng and R. Allen, "Evaluation of the effects of the communication cable on the dynamics of an underwater flight vehicle," *Ocean Engineering*, 31, pp. 1019-1035, 2004.
- [4] D. Hopkin, M. Davis and I. Gartshore, "The aerodynamics and control of a remotely-piloted underwater towed vehicle," *Canadian Aeronautics and Space Journal*, vol. 36, no. 3, pp. 122-129, 1990.
- [5] F. S. Hover and D. R. Yoerger, "Identification of low-order dynamic models for deeply-towed underwater vehicle systems," *Proc. First Int. Offshore Polar Eng. Conf.*, pp. 97-105, 1991.
- [6] S. Huang, "Dynamic analysis of three-dimensional marine cables," *Ocean Engineering*, vol. 21, no. 6, pp. 587-605, 1994.
- [7] I. W. Kamman, S. D. Patek and S. A. Hoeckley, "Application of Multivariable linear control design to marine towed systems," *J. Guidance, Control and Dynamics*, vol. 19, no. 6, pp. 1246-1251, 1996.
- [8] N. Kato, "Underwater towed vehicle maneuverable in both vertical and horizontal axis (Part I: Principal configuration and attitude control)," *Journal of the Society of Naval Architects of Japan*, no. 169, pp. 111-122, 1991.
- [9] N. Kato, "Guidance and control of underwater towed vehicle maneuverable in both vertical and horizontal axis," *Proc. Second Int. Offshore Polar Eng. Conf.*, pp. 505-512, 1992.
- [10] C. Lambert, M. Nahon, B. Buckham, and M. Seto, "Dynamics and control of a towed underwater vehicle system, part II: model validation and turn maneuver optimization," *Ocean Engineering*, 30, pp. 471-485, 2003.
- [11] B. C. Moore, "Principal component analysis in linear systems: controllability, observability, and model reduction," *IEEE Trans. AC*, vol. 26, no. 1, pp. 17-32, 1981.
- [12] J. N. Newman, *Marine Hydrodynamics*. Cambridge, MA: MIT Press, 1977.
- [13] H. Nijmeijer and A. J. van der Schaft, *Nonlinear Dynamical Control Systems*. New York, NY: Springer-Verlag, 1990.
- [14] D. Perrault, G. Hackett and M. Nahon, "Simulation and active control of towed undersea vehicles," *Proc. Oceans '97*, pp. 1277-1282, 1997.
- [15] T. S. Walton and H. Polachek, "Calculation of transient motion of submerged cables," *Mathematics of computation*, 14, pp. 27-46, 1960.
- [16] W. M. Wonham, *Linear Multivariable Control: A Geometric Approach*. Berlin, Springer-Verlag, 1974.
- [17] T. Yokobiki, W. Koterayama, S. Yamaguchi, and M. Nakamura, "Dynamics and control of a towed vehicle in transient mode," *Int. J. of Offshore and Polar Engineering*, vol. 10, no. 1, pp. 19-25, 2000.